We propose that oxidative addition to the 17-electron radical occurs to form, transiently, a 19-electron product which rapidly loses CO, eq 17. The product $CpW(CO)_2(Sn(n\text{-}Bu_3)(H)$ is also

$$CpW(CO)_3 + (n\text{-}Bu)_3SnH \xrightarrow{rds} CpW(CO)_3(Sn(n\text{-}Bu)_3)(H) \xrightarrow{fast} CpW(CO)_2(Sn(n\text{-}Bu)_3)(H) + CO \quad (17)$$

a 17-electron radical and may abstract H from $(n\text{-}Bu)_3SnH$.[97] This reaction occurs after the rate-determining step; therefore, no information about it can be obtained from the kinetic data.

Chain Reactions. For some organic halides, such as CHI_3, Ph_3CBr, and $BrCH_2CH_2CN$, as well as for $BrCo(dmgH)_2PPh_3$, $(n\text{-}Bu)_3SnI$, and O_2, high concentrations gave postflash loss of dimer absorbance, shown for O_2 in Figure 6b. The concentration of oxidant required to observe dimer loss rather than radical recombination (dimer recovery) was $[ox] > 10^5/k_X$. Our observations are consistent with the onset of a chain reaction in which organic and organometallic radicals are chain carriers. A possible mechanism is shown in Scheme I. When the rate of reaction 18

Scheme I

$$CpW(CO)_3 + RX \rightarrow CpW(CO)_3X + R^\cdot \quad (18)$$

$$R^\cdot + [CpW(CO)_3]_2 \rightarrow R^+ + CpW(CO)_3^- + CpW(CO)_3 \quad (19)$$

is large (high [RX]), a high concentration of $[R^\cdot]$ is produced. Consequently, enough $R^\cdot$ proceeds by reaction 19 (even though radical coupling is simultaneously enhanced) to make loss of the dimer $[CpW(CO)_3]_2$ significant. A similar scheme can be written with superoxide (free or coordinated to $CpW(CO)_3^+$) or Co(II)$(dmgH)_2PPh_3$ as the species which reduces $[CpW(CO)_3]_2$. Further studies of the mechanisms of these photoinitiated chain reactions are in progress.

Acknowledgment. We thank Professor R. J. Angelici and his students for a gift of $[CpW(CO)_3]_2$. This work was supported by the U.S. Department of Energy, Office of Basic Energy Sciences, Chemical Sciences Division, under Contract W-7405-Eng-82.

Ligand Conformational Changes Affecting $^5T_2 \rightarrow {}^1A_1$ Intersystem Crossing in a Ferrous Complex

James K. McCusker,[1] Hans Toftlund,[2] Arnold L. Rheingold,[3] and David N. Hendrickson*,[1]

Contribution from the Department of Chemistry-0506, University of California at San Diego, La Jolla, California 92093-0506, Department of Chemistry, University of Odense, DK-5230 Odense M, Denmark, and Department of Chemistry, University of Delaware, Newark, Delaware 19716. *Received July 27, 1992*

Abstract: Results are presented from a variable-temperature solution-phase laser photolysis study of the $^5T_2 \rightarrow {}^1A_1$ intersystem crossing in $[Fe(t\text{-tpchxn})](ClO_4)_2$, where the hexadentate ligand *t*-tpchxn is *trans*-1,2-bis(bis(2-pyridylmethyl)amino)cyclohexane. The complex $[Fe(t\text{-tpchxn})](ClO_4)_2 \cdot H_2O \cdot CH_3OH$ crystallizes in the space group $P2_12_12_1$, which at 299 K has a unit cell with $a = 9.565(4)$ Å, $b = 13.178(5)$ Å, $c = 27.276(23)$ Å, and $Z = 4$. Refinement with 1905 observed $[F > 3.0\sigma(F)]$ reflections gave $R = 0.0924$ and $R_w = 0.1147$. The structure indicates that the complex has spontaneously resolved into optically pure crystals. After excitation into a $^1MLCT \leftarrow {}^1A_1$ band ($\lambda_{pump} = 440$ nm), relaxation profiles were determined at 420 nm for a CH_3OH solution of $[Fe(t\text{-tpchxn})](ClO_4)_2$ in the range 191–280 K. In the range 190–250 K, the compound exhibits biphasic relaxation kinetics, whereas a single-exponential model was adequate from 260 to 280 K. From plots of $\ln(k)$ versus $1/T$ for each of the two relaxation processes in the 190–250 K range, activation parameters and frequency factors were found to be 964 ± 23 cm^{-1} and $(3.7 \pm 0.5) \times 10^9$ s^{-1}, respectively, for the τ_1 process and 2370 ± 60 cm^{-1} and $(5 \pm 2) \times 10^{12}$ s^{-1}, respectively, for the τ_2 process ($\tau_1 < \tau_2$). The observation of *two* relaxation processes for $[Fe(t\text{-tpchxn})](ClO_4)_2$ in CH_3OH stands in contrast to the data reported previously for the same complex in either DMF or CH_3CN, where in both solvents only a single-exponential relaxation profile is seen. Both of the relaxation processes observed for the methanol solution are assigned as $^5T_2 \rightarrow {}^1A_1$ intersystem crossing processes. It is suggested that $[Fe(t\text{-tpchxn})]^{2+}$ undergoes a solvent-induced conformational change of the cyclohexyl ring, giving rise to two different high-spin forms of the complex having different spin-state interconversion dynamics.

Introduction

A spin-crossover complex has a low-energy excited electronic state which can be thermally populated.[4] The factors which affect the rate of intersystem crossing between the low-spin ($^1A_1$) and high-spin ($^5T_2$) states of ferrous spin-crossover complexes are being studied for a variety of reasons.[5] Apart from fundamental interest in the dynamics of intersystem crossing processes, transition metal sites in metalloenzymes catalyze the reaction of paramagnetic O_2 with diamagnetic organic substrates. In fact, spin-state changes occurring at metal sites in proteins can be rate controlling in the functioning of certain metalloenzymes, e.g., mammalian P450.[6] Finally, intersystem crossing rates in Fe^{II} complexes are being studied in order to understand the LIESST (light-induced excited-spin-state trapping) effect discovered by Gütlich et al.[7] In

(1) University of California at San Diego.
(2) University of Odense.
(3) University of Delaware.
(4) (a) Toftlund, H. *Coord. Chem. Rev.* **1989**, *94*, 67. (b) Kõnig, E. *Prog. Inorg. Chem.* **1987**, *35*, 527–622. (c) Gütlich, P. *Struct. Bonding (Berlin)* **1981**, *44*, 83. (d) Goodwin, H. A. *Coord. Chem. Rev.* **1976**, *18*, 293. (e) Scheidt, W. R.; Reed, C. A. *Chem. Rev.* **1981**, *81*, 543. (f) König, E.; Ritter, G.; Kulshreshtha, S. K. *Chem. Rev.* **1985**, *85*, 219. (g) Bacci, M. *Coord. Chem. Rev.* **1988**, *86*, 245. (h) Gütlich, P. In *Chemical Mõssbauer Spectroscopy*; Herber, R. H., Ed.; Plenum Press: New York, 1984. (i) Maeda, Y.; Takashima, Y. *Comments Inorg. Chem.* **1988**, *7*, 41. (j) Gütlich, P.; Hauser, A. *Coord. Chem. Rev.* **1990**, *97*, 1–22.
(5) Beattie, J. K. *Adv. Inorg. Chem.* **1988**, *32*, 1–53.
(6) Fisher, M. T.; Sligar, S. G. *Biochemistry* **1987**, *26*, 4797–4803. (b) Backes, W. L.; Sligar, S. G.; Schenkman, J. B. *Biochemistry* **1982**, *21*, 1324–13330. (c) Tamburini, P. P.; Gibson, G. G.; Backes, W. L.; Sligar, S. G.; Schenkman, J. B. *Biochemistry* **1984**, *23*, 4526–4533.
(7) (a) Decurtins, S.; Gütlich, P.; Kohler, C. P.; Spiering, H.; Hauser, A. *Chem. Phys. Lett.* **1984**, *105*, 1. (b) Decurtins, S.; Gütlich, P.; Kohler, C. P.; Spiering, H. *J. Chem. Soc., Chem. Commun.* **1985**, 430. (c) Decurtins, S.; Gütlich, P.; Hasselbach, K. M.; Hauser, A.; Spiering, H. *Inorg. Chem.* **1985**, *24*, 2174. (d) Poganuich, P.; Decurtins, S.; Gütlich, P. *J. Am. Chem. Soc.* **1990**, *112*, 3270–3278. (e) Kahn, O.; Launay, J. P. *Chemtronics* **1988**, *3*, 140–151.

0002-7863/93/1515-1797$04.00/0

this phenomenon, solid samples of Fe^{II} spin-crossover complexes maintained at low temperatures can be optically driven back and forth between the stable $^1A_1$ form and the metastable $^5T_2$ form.

McGarvey and Lawthers[8] were the first to employ the laser-flash photolysis technique to directly measure the rate at which spin-crossover complexes interconvert between the $^5T_2$ and $^1A_1$ states. Several other laser-flash studies followed.[9] The temperature dependence of the $^5T_2 \rightarrow {}^1A_1$ relaxation has been measured for several Fe^{II} spin-crossover complexes both in solution and in the solid state.[10] In the latter case, the temperature dependence has been measured from 300 to 4.2 K. At temperatures below 150 K, several complexes exhibit a temperature-independent rate of $^5T_2 \rightarrow {}^1A_1$ interconversion which has been taken as evidence of tunneling.[10]

Very recently we employed[11] variable-temperature laser photolysis to study the $^5T_2 \rightarrow {}^1A_1$ intersystem crossing dynamics of polypyridyl Fe^{II} complexes such as $[Fe(terpy)_2](ClO_4)_2$ and $[Fe(tpen)](ClO_4)_2$, where terpy is terpyridine and tpen is the following hexadentate ligand:

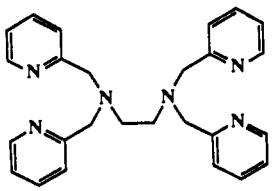

(tpen)

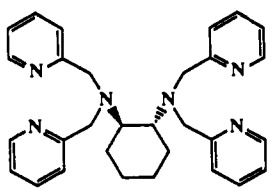

(*t*-tpchxn)

The ethylenediamine moiety in tpen was changed to various diamine units to examine whether a torsional distortion imparted by the tpen-type hexadentate ligand affected the kinetics of the $^5T_2 \rightarrow {}^1A_1$ intersystem crossing. Fitting of the temperature-dependence data measured for several tpen-type Fe^{II} complexes in solution to classical, semiclassical, and quantum-mechanical expressions for interconversion between two weakly coupled states indicated that the kinetics cannot be described by coupling to the metal–ligand stretching mode in a single configurational coordinate model. Rather, the data are consistent with coupling to low-frequency (<90 cm^{-1}) modes, suggesting kinetic control via torsional coordinates.

In this paper, some unusual results for the spin-crossover complex $[Fe(t\text{-tpchxn})](ClO_4)_2$ are reported. It will be shown that $[Fe(t\text{-tpchxn})]^{2+}$ shows two relaxation processes following $^1MLCT \leftarrow {}^1A_1$ excitation. This is in contrast to all other Fe^{II} complexes studied to date, which exhibit only one relaxation process. McGarvey et al.[12] have previously studied the spin-state interconversion kinetics of $[Fe(t\text{-tpchxn})](ClO_4)_2$ as a function of both temperature and pressure in DMF and CH_3CN (vide infra). Two quite different activation enthalpies were found for the complex in the two solvents. From the pressure studies, they found an activation volume of $\Delta V^{\ddagger} = -6.1 \pm 1.2$ cm^3 mol^{-1} in CH_3CN and $+5.7 \pm 1.0$ cm^3 mol^{-1} in DMF. The positive value for $\Delta V^{\ddagger}$ in DMF is unusual. Our results support their suggestion that the solvent is influencing the dynamics of spin-state interconversion in this complex.

Experimental Section

Compound Preparations. All materials were of reagent grade and were used without further purification unless otherwise indicated. $FeCl_2 \cdot 2H_2O$ was freshly prepared from $FeCl_2 \cdot 4H_2O$ (Fisher), Fe powder, and HCl as previously described.[11] All manipulations with solutions containing Fe^{II} were performed under an inert atmosphere of N_2 using standard Schlenk techniques. The racemic form of the pure ligand *t*-tpchxn was prepared by a modification of a previously reported procedure.[13]

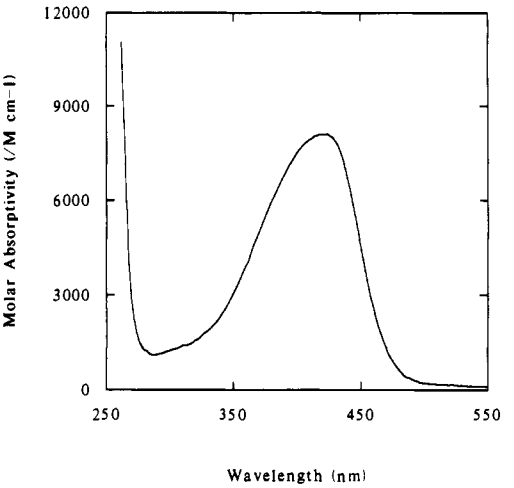

Figure 1. Electronic absorption spectrum of $[Fe(t\text{-tpchxn})](ClO_4)_2$ in MeOH solution in the region of the $^1MLCT \leftarrow {}^1A_1$ transition.

Table I. Crystallographic Data for $[Fe(t\text{-tpchxn})](ClO_4)_2 \cdot H_2O \cdot CH_3OH$

$C_{31}H_{40}Cl_2FeN_6O_{10}$	$P2_12_12_1$
fw = 783.4	T = 299 K
a = 9.565(4) Å	λ = 0.71703 Å
b = 13.178(5) Å	ρ_{calcd} = 1.514 g cm^{-3}
c = 27.276(23) Å	μ = 6.60 cm^{-1}
V = 3438.1 Å^3	R^a = 0.0924
Z = 4	$R_w{}^a$ = 0.1147

$^a R = \sum||F_o| - |F_c|/\sum|F_o|$; $R_w = [\sum w(|F_o| - |F_c|)^2/[\sum w|F_o|^2]^{1/2}$.

Synthesis of $[Fe(t\text{-tpchxn})](ClO_4)_2$. The racemic form of the free ligand *t*-tpchxn (0.088 g, 0.18 mmol) was dissolved in 20 mL of MeOH, and the solution was pumped and purged with N_2. To this stirred solution was added an aqueous solution of $FeCl_2 \cdot 2H_2O$ (0.030 g, 0.18 mmol in 3 mL of deoxygenated H_2O), resulting in the immediate formation of a clear, red reaction mixture. This solution was gently heated to ca. 50 °C for 2 h, after which $NaClO_4$ (0.050 g, 0.36 mmol in 5 mL of deoxygenated H_2O) was added in a dropwise fashion. Complete addition of the $NaClO_4$(aq) solution produced no noticeable change in the appearance of the reaction mixture. The heat was removed, and the solution was slowly concentrated by passing a stream of N_2 over the top of the solution. A crystalline product was isolated by filtration after 1 day of slow evaporation. The crystals used in the X-ray study were selected from this sample. The optical spectrum of the compound (Figure 1) is identical to that reported in the literature.[13] The crystal structure confirms the formulation of the compound as a solvate, $[Fe(\pm t\text{-tpchxn})](ClO_4)_2 \cdot H_2O \cdot CH_3OH$. Anal. Calcd for $FeC_{31}H_{43}N_6Cl_2O_{10.5}$: C, 45.94; H, 5.35; N, 10.37; Fe, 6.89. Found: C, 46.23; H, 4.93; N, 10.44; Fe, 7.26. (Note: the elemental analysis was performed on a ground sample that had picked up additional H_2O relative to the single crystal used in the X-ray study.)

Physical Measurements. Optical spectra were recorded using a Hewlett-Packard HP8452A diode array spectrophotometer. Each reported spectrum represents a signal average of 250 spectra collected in 0.1-s intervals with the sample maintained at ambient temperature (ca. 295 K). Magnetic susceptibility data were collected on a ground solid sample of $[Fe(\pm t\text{-tpchxn})](ClO_4)_2$ in an applied field of 10.0 kG using a SQUID susceptometer (Quantum Design MPMS, San Diego, CA). Diamagnetic corrections for the molecule were made using Pascal's constants, whereas corrections for the sample holder were made by measuring the susceptibility of an empty sample holder and subtracting this value from the raw magnetization data on the compound. Laser photolysis experiments were carried out using a nanosecond time-resolved spectrometer as previously described.[11]

X-ray Crystallography. A red crystal was mounted with epoxy cement on a glass fiber. Systematic absences in the diffraction data uniquely determined the orthorhombic space group $P2_12_12_1$. No correction for absorption was required. The data were collected to the maximum 2θ limit of the observed data. The structure was solved by a combination

(8) McGarvey, J. J.; Lawthers, I. *J. Chem. Soc., Chem. Commun.* **1982**, 906.

(9) (a) Lawthers, I.; McGarvey, J. J. *J. Am. Chem. Soc.* **1984**, *106*, 4280. (b) McGarvey, J. J.; Lawthers, I.; Toftlund, H. *J. Chem. Soc., Chem. Commun.* **1984**, 1576.

(10) (a) Xie, C.-L.; Hendrickson, D. N. *J. Am. Chem. Soc.* **1987**, *109*, 6981–6988. (b) Conti, A. J.; Xie, C.-L.; Hendrickson, D. N. *J. Am. Chem. Soc.* **1989**, *111*, 1171–1180.

(11) McCusker, J. K.; Hendrickson, D. N. Submitted for publication.

(12) McGarvey, J. J.; Lawthers, I.; Heremans, K.; Toftlund, H. *Inorg. Chem.* **1990**, *29*, 252.

(13) Toftlund, H.; Yde-Andersen, S. *Acta Chem. Scand.* **1981**, *A35*, 575.

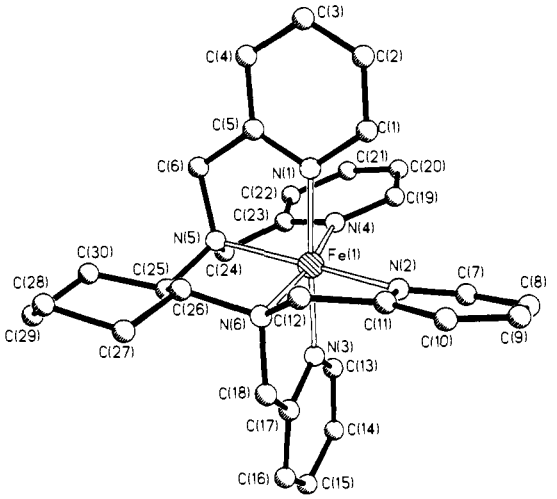

Figure 2. Structure of the cation of $[Fe(t\text{-tpchxn})](ClO_4)_2$ based on a single-crystal X-ray structure.

of direct methods and difference Fourier syntheses. Due to restrictions in the available data, only atoms heavier than carbon were anisotropically refined. Hydrogen atoms were placed in fixed, idealized locations. The "hand" was determined by the refinement of a multiplicative term for $\Delta f''$ which refined to 1.07(4), indicating that the reported hand is correct. All computations used SHELXTL PC software (G. Sheldrick, Siemens XRD, Madison, WI). Details of the data collection are summarized in Table I.

Results and Discussion

Crystal Structure of $[Fe(\pm t\text{-tpchxn})](ClO_4)_2$. Slow evaporation of a reaction mixture containing $\pm t$-tpchxn, $FeCl_2$, and $NaClO_4$ in $MeOH/H_2O$ afforded X-ray-quality crystals of the perchlorate salt of $[Fe(t\text{-tpchxn})]^{2+}$. The molecule crystallizes as a H_2O/MeOH solvate in the orthorhombic space group $P2_12_12_1$ with $Z = 4$. The pertinent crystallographic details of the data collection are given in Table I. A computer-generated drawing of the cation is illustrated in Figure 2. Since we started with a racemic mixture of the ligand, the crystal structure indicates that the complex has spontaneously resolved into its optical isomers upon crystallization. This is a rather rare phenomenon, but it is by no means unprecedented.[14] In fact, this is the second molecule in this general series of polypyridyl ligands that has been found to spontaneously resolve. The other complex, $[Fe(tptcn)](ClO_4)_2$, crystallizing in the trigonal space group $P3$, was described by Christiansen et al.[14a] The absolute configuration of the cation of $[Fe(t\text{-tpchxn})](ClO_4)_2$ for the particular crystal chosen for the X-ray study is Λ; it is assumed that the Δ isomer is also formed and could be characterized given another crystal.

Selected bond distances and angles are listed in Table II with anisotropic thermal parameters and calculated hydrogen atom positions given in tables in the supplementary material. The coordination sphere about the Fe^{II} ion is a distorted octahedron with ligation from the two tertiary amines of the *trans*-1,2-diaminocyclohexylene ring and four aromatic nitrogen atoms from the pendant pyridylmethyl arms of the ligand. Both the $Fe-N_{aliph}$ bond distances (average 1.995 ± 0.005 Å) and the $Fe-N_{py}$ bond distances (average 2.005 ± 0.016 Å) are somewhat long for low-spin Fe^{II}, suggesting that there is some high-spin contribution to the observed structure[15] of this compound at 299 K (vide infra). Bond distances within the pyridine rings are unremarkable, with

Table II. Selected Bond Distances and Angles for $[Fe(t\text{-tpchxn})](ClO_4)_2 \cdot H_2O \cdot CH_3OH$

	Bond Distances (Å)		
Fe(1)–N(1)	1.993(13)	Fe(1)–N(2)	2.003(13)
Fe(1)–N(3)	1.992(13)	Fe(1)–N(4)	1.992(13)
Fe(1)–N(5)	2.012(13)	Fe(1)–N(6)	2.038(13)
	Bond Angles (deg)		
N(1)–Fe(1)–N(2)	89.2(5)	N(1)–Fe(1)–N(3)	177.1(5)
N(2)–Fe(1)–N(3)	89.9(5)	N(1)–Fe(1)–N(4)	86.8(5)
N(2)–Fe(1)–N(4)	111.8(5)	N(3)–Fe(1)–N(4)	91.0(5)
N(1)–Fe(1)–N(5)	84.9(5)	N(2)–Fe(1)–N(5)	165.2(6)
N(3)–Fe(1)–N(5)	96.6(5)	N(4)–Fe(1)–N(5)	81.4(6)
N(1)–Fe(1)–N(6)	96.9(5)	N(2)–Fe(1)–N(6)	80.3(5)
N(3)–Fe(1)–N(6)	85.6(5)	N(4)–Fe(1)–N(6)	167.4(6)
N(5)–Fe(1)–N(6)	86.9(6)		

an average C–C distance of 1.38 ± 0.03 Å and a C–N distance of 1.36 ± 0.02 Å for all four rings. The cyclohexylene ring is also relatively unperturbed upon complexation to the metal in terms of internal C–C bond distances and angles. The equatorial[16] pyridine rings are tilted at an angle of 14.4(1)° relative to each other as described by the N(4)···C(21) and N(2)···C(9) vectors, while the axial rings are nearly perpendicular at an angle of ca. 85°. This canting of the axial pyridine rings does not appear to significantly affect the relative positions of the two rings with respect to the octahedron, since the N(1)–Fe–N(3) bond angle of 177.1(5)° is fairly close to the expected value of 180°.

The most interesting aspect of the structure of $[Fe(t\text{-tpchxn})]^{2+}$ is the cyclohexylene ring. The ring is in a perfect chair conformation as evidenced by a C(27)–C(28)–C(29)–C(30) dihedral angle of 59.7(5)°, a number identical within experimental error to the value of 60° expected for cyclohexane. The geometries about the trans amino groups are reasonably close to tetrahedral with bond angles ranging from 103.4(1) to 113.6(1)° at N(5) and from 105.5(9) to 113.5(1)° at N(6). Surprisingly, the five-membered ring that arises due to chelation of the 1,2-diamino groups to the metal also exhibits a near-perfect chair structure, with a N(5)–C(25)–C(26)–N(6) dihedral angle of 61.3(5)°. This latter result is remarkable if one examines the dihedral angles of the four other five-membered chelate rings in the molecule. For example, the equatorial chelate rings are characterized by dihedral angles of 29.6° [N(2)–C(11)–C(12)–N(6)] and 33.0° [N(4)–C(23)–C(24)–N(5)], whereas the axial chelate rings exhibit even smaller distortions from planarity at 4.9° [N(1)–C(5)–C(6)–N(5)] and 14.0° [N(3)–C(17)–C(18)–N(6)]. This wide range in dihedral angles and the strain introduced by the linking of four fused chelate rings no doubt contribute to the significant deviations from the expected 90° angles for the cis ligations in the coordination sphere of the metal. Values for these angles range from 111.8(5)° for N(2)–Fe–N(4) down to 80.3(5)° for N(2)–Fe–N(6). It is likely that the two equatorial and two axial chelate rings are distorting in order to accommodate the trans configuration of the 1,2-diamino group and its preference for a ~60° N(5)–C(25)–C(26)–N(6) dihedral angle upon complexation. The conformation of the *trans*-1,2-diaminocyclohexylene moiety is probably the dominant structural influence in the coordination sphere of the metal.

The molecule crystallizes with 1 equiv each of H_2O and CH_3OH per formula unit. Although no protons were experimentally located in the structure, their positions were calculated using a molecular modeling program[17] to get a rough estimate of the nearest-neighbor contacts between the solvate molecules and $[Fe(t\text{-tpchxn})](ClO_4)_2$. The H_2O molecule resides closest to the cyclohexylene ring of $[Fe(t\text{-tpchxn})]^{2+}$ with a 2.8-Å van der Waals distance between the oxygen [O(9)] and the axial proton on C(30). The oxygen atom of the CH_3OH molecule [O(10)] is calculated to be 2.8 Å from the hydrogen atoms on C(12). The shortest van

(14) (a) Christiansen, L.; Hendrickson, D. N.; Toftlund, H.; Wilson, S. R.; Xie, C.-L. *Inorg. Chem.* **1986**, *25*, 2813. (b) For more information on the crystallographic resolution of optical isomers, see: Stout, G. H.; Jensen, L. H. *X-Ray Structure Determination, A Practical Guide*, 2nd ed.; John Wiley and Sons, Inc.: New York, 1989; pp 410–412.

(15) Since single-crystal X-ray data are collected over a period of many hours, the structure obtained will reflect the average of any distributions or dynamics that may be present in the lattice. For spin-crossover molecules, the result is a structure that represents a weighted average of the high-spin/low-spin ratio present at the temperature at which the data were collected.

(16) For the purposes of this discussion, we define the equatorial plane as the plane containing the cyclohexylene ring.

(17) INSIGHT II, A Molecular Modeling Program, Biosym Technologies, Inc., San Diego, CA.

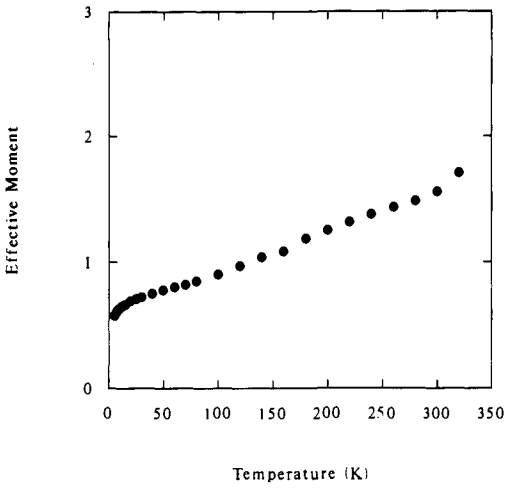

Figure 3. Plot of the effective magnetic moment (μ_{eff}) of a powdered sample of [Fe(t-tpchxn)](ClO$_4$)$_2$ as a function of temperature.

der Waals contact (1.6 Å) was found between the hydrogens of the methyl group of the solvate [C(31)] and the equatorial proton on C(27). Aside from these, there does not appear to be any significant interaction between the solvate molecules and either the [Fe(t-tpchxn)]$^{2+}$ cation or the perchlorate anions.

Spin-Crossover Behavior of [Fe(t-tpchxn)](ClO$_4$)$_2$. The magnetic properties of [Fe(t-tpchxn)](ClO$_4$)$_2$ have been previously reported elsewhere by Toftlund and co-workers.[4a,12,13] The complex when crystallized as a $2H_2O$ solvate[13] has an effective moment of 1.15 μ_B at 305 K, corresponding to a high-spin $\rightleftharpoons$ low-spin equilibrium constant of 0.03 as calculated by eq 1, where χ_m is

$$K_{eq} = \frac{\chi_m - \chi_{ls}}{\chi_{hs} - \chi_m} \quad (1)$$

the measured susceptibility, χ_{ls} is the susceptibility of the pure low-spin form of the complex, and χ_{hs} is the susceptibility of the pure high-spin form. The values for χ_{ls} and χ_{hs} were taken from magnetic data[11] on [Fe(mtpen)](ClO$_4$)$_2$ and [Fe(tptn)](ClO$_4$)$_2$, which are high-spin and low-spin complexes, respectively. We have determined the magnetic susceptibility in the 5.01–320.0 K range of our sample isolated as a H_2O/CH_3OH solvate; these data are given in the supplementary material and plotted as μ_{eff} versus temperature in Figure 3. The data are characteristic of a spin-crossover molecule showing an increase in effective moment with increasing temperature. The effective moment for [Fe(t-tpchxn)](ClO$_4$)$_2$·H_2O·CH_3OH at 300 K is ~1.5 μ_B, indicating that there is some high-spin population in the solid-state at this temperature. This result explains the long "low-spin" Fe^{II}–N bond lengths observed in the X-ray structure at 299 K. The fact that our data differ slightly from those of Toftlund and Yde-Andersen[13] is not too surprising, since it is well-known that the presence of lattice solvate molecules can have a significant impact on spin-crossover behavior in the solid state.[4]

For the purposes of our laser photolysis studies, the magnetic properties of [Fe(t-tpchxn)](ClO$_4$)$_2$·S in the solid are not of great concern, since the kinetic measurements were made in solution. Toftlund and co-workers have done extensive work on measuring the magnetic susceptibility of [Fe(t-tpchxn)](ClO$_4$)$_2$ (among other compounds) in both DMF and CH_3CN solutions.[4a,12] The spin equilibrium of [Fe(t-tpchxn)](ClO$_4$)$_2$ has been found to be solvent-dependent, exhibiting quite different thermodynamic properties in DMF and CH_3CN. On the basis of plots of ln(K_{eq}) versus T^{-1}, Toftlund and co-workers have determined values for the standard enthalpy of the spin equilibrium (ΔH_0) of 23.6 and 24.4 kJ mol^{-1} in DMF and CH_3CN, respectively, and ΔS_0 values of 64.9 and 75.3 J K^{-1} mol^{-1}, respectively. These thermodynamic parameters translate into critical temperatures (T_c, K_{eq} = 1) of ~365 K (DMF) and ~340 K (CH_3CN). We have *not* examined the solution susceptibility of [Fe(t-tpchxn)](ClO$_4$)$_2$ in CH_3OH, the solvent we have chosen to perform our kinetic studies in. This type of a measurement needs to be made to take full advantage of the relaxation data obtained as a function of temperature (vide infra). With the general trend of low-spin stabilization with increasing solvent polarity, we would expect on the basis of Toftlund's results in DMF and CH_3CN that a CH_3OH solution of [Fe(t-tpchxn)](ClO$_4$)$_2$ will exhibit a T_c of ~350 K. This corresponds to a zero-point energy difference between the $^1A_1$ and $^5T_2$ states (ΔE_0) of approximately 400 cm^{-1}. Toftlund has reported magnetic data on [Fe(t-tpchxn)](ClO$_4$)$_2$ in H_2O/2-methoxyethanol solution (1:1 v/v) in the form of a plot of μ_{eff} vs temperature.[4a] Graphical inspection reveals that the data are very similar to those for solutions of [Fe(tpen)](ClO$_4$)$_2$ in the same solvent; the T_c for [Fe(tpen)](ClO$_4$)$_2$ under those conditions is 356 K.

Relaxation Kinetics of [Fe(t-tpchxn)](ClO$_4$)$_2$. Before we describe our results, it is useful to review kinetic data reported earlier on the same complex. The spin-state interconversion kinetics of [Fe(t-tpchxn)](ClO$_4$)$_2$ have been studied previously by McGarvey et al.[12] as a function of both temperature and pressure. The technique employed was laser photolysis with excitation at several wavelengths (e.g., 532, 416, 354.7 nm) and probing in the ^{1}MLCT $\leftarrow$ $^1A_1$ absorption band. Relaxation kinetics were reported to be independent of pump and probe wavelengths and of concentration over the temperature range studied (240–300 K). In DMF solution, an activation enthalpy of $\Delta H^{\ddagger}$ = 34.4 ± 1.2 kJ mol^{-1} (2880 cm^{-1}) was found, while a value of only 1.8 kJ mol^{-1} (150 cm^{-1}) was observed in CH_3CN.

Even more striking than the difference in activation energy as a function of solvent are the data from the variable-pressure studies. A change in molecular volume occurs in spin-crossover systems due to the large change in metal–ligand bond lengths that accompanies the transition. This volume change means that the relaxation induced by perturbations (e.g., laser photolysis) can be studied as a function of static pressure to determine the activation volume for the spin transition. If we interpret the activation volume as the change in molecular volume on going from the initial state to the transition state,[18] it is reasonable to anticipate that the high-spin $\rightarrow$ low-spin conversion will be characterized by a negative value for $\Delta V^{\ddagger}$, i.e., contraction of the complex from the high-spin state to the transition state. Admittedly, this is an overly simplistic viewpoint, since the observed activation volume will be the result of contributions from both internal and external factors such that $\Delta V_{obs}^{\ddagger} = \Delta V_{int}^{\ddagger} + \Delta V_{ext}^{\ddagger}$. The external component is largely due to changes in the solvation shell on forming the transition state, and whether this term will be positive or negative is difficult to predict. However, our simple expectations are borne out by experiment: in *almost* every case the activation volume for the $^5T_2 \rightarrow {}^1A_1$ spin conversion is found to be negative. For example, [Fe(t-tpchxn)](ClO$_4$)$_2$ in CH_3CN is reported by McGarvey et al.[12] to have $\Delta V^{\ddagger}$ = −6.1 ± 1.2 cm^3 mol^{-1}. This value is within the typical range found for ferrous spin-crossover complexes.[19] Actually, the quite narrow range of $\Delta V^{\ddagger}$ values found for the $^5T_2 \rightarrow {}^1A_1$ conversion in Fe^{II} complexes is often interpreted[12] as indicating that the primary contribution to the activation volume is intramolecular and that the $^5T_2$ state and the transition state are solvated to a similar extent.

The trend of negative values for $\Delta V^{\ddagger}$ is broken with [Fe(t-tpchxn)](ClO$_4$)$_2$ in DMF solution: McGarvey et al.[12] give for this sample $\Delta V^{\ddagger}$ = +5.7 ± 2.0 cm^3 mol^{-1}. The *positive* value for the activation volume stands in stark contrast to the results obtained on every other spin-crossover system studied and suggests an expansion of the molecular unit upon forming the transition state from the $^5T_2$ state. Furthermore, the difference in activation volumes between [Fe(t-tpchxn)](ClO$_4$)$_2$ in CH_3CN and DMF suggests that the mechanism of the $^5T_2 \rightarrow {}^1A_1$ conversion is different in the two solvents and is therefore solvent-dependent. This result at least qualitatively explains why such a large dif-

(18) We point out that while an activation volume has this very straightforward physical interpretation in the context of transition state theory, its meaning within a quantum-mechanical framework is not at all obvious.

(19) König, E. *Struct. Bonding (Berlin)* **1991**, *76*, 51.

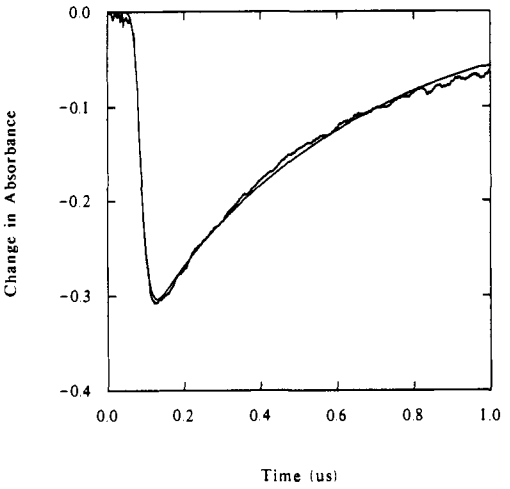

Figure 4. Transient decay profile of $[Fe(t\text{-tpchxn})](ClO_4)_2$ in CH_3OH (2.51×10^{-4} M) at 420 nm following excitation at 440 nm. Data were collected at 191 K. The smooth solid line represents a convolution of the instrument response function with a single-exponential decay, τ_{obs} = 547 ns.

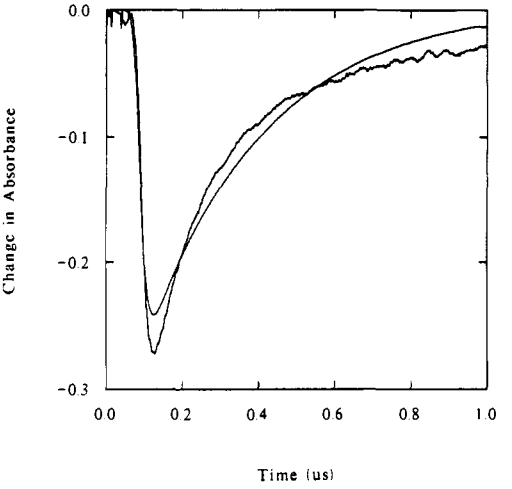

Figure 5. Transient decay profile of $[Fe(t\text{-tpchxn})](ClO_4)_2$ in CH_3OH (2.51×10^{-4} M) at 420 nm following excitation at 440 nm. Data were collected at 225 K. The smooth solid line represents a convolution of the instrument response function with a single-exponential decay, τ_{obs} = 314 ns.

ference in activation enthalpies was observed between the DMF and CH_3CN data in the variable-temperature studies. McGarvey et al.[12] suggested that the positive value for $\Delta V^{\ddagger}$ supports a torsional mode for the molecular mechanism of spin-state interconversion. They proposed that the fused backbone of the cyclohexylene ring blocks the preferred rhombic twist motion of the molecule and causes the system to proceed by a higher-energy (i.e, $\Delta H^{\ddagger}$ = 2880 cm^{-1} versus 150 cm^{-1}) radial expansion mode. In their model, then, a negative value of $\Delta V^{\ddagger}$ indicates coupling to the "normal" reaction coordinate that is dominated by a low-energy torsional mode. The observation of $\Delta V^{\ddagger} > 0$ for a DMF solution of $[Fe(t\text{-tpchxn})](ClO_4)_2$ represents a steric block to torsional motion, causing the system to convert along a predominantly radial path. Their proposal was supported by angular overlap model calculations and a semiquantitative potential energy surface, reinforcing the ideas of Purcell[20] that torsional motion lowers the energy of the intermediate S = 1 state(s) necessary for spin–orbit mixing of the S = 0 and S = 2 spin manifolds. Radial expansion of the coordination sphere, in addition to involving higher-energy normal modes of the molecule, does not induce stabilization of the S = 1 manifold. The result is a higher-energy pathway for spin-state interconversion.

We collected variable-temperature relaxation data on a 2.51 $\times 10^{-4}$ M (3.18×10^{-4} *m*) CH_3OH solution of $[Fe(t\text{-tpchxn})](ClO_4)_2$. A transient decay profile (λ_{probe} = 420 nm) collected on $[Fe(t\text{-tpchxn})](ClO_4)_2$ at 191 K following excitation at λ_{pump} = 440 nm is illustrated in Figure 4. The smooth solid line is the best fit to a single-exponential decay, fit via convolution with the instrument response function. Although the fit is not too bad, it does not exhibit quite the same level of quality as fits found[11] for other complexes such as $[Fe(tpen)](ClO_4)_2$. The hint that a single-exponential decay model is not sufficient to describe the relaxation kinetics of $[Fe(t\text{-tpchxn})](ClO_4)_2$ is confirmed upon increasing the temperature. In Figure 5 is plotted the transient absorbance decay of $[Fe(t\text{-tpchxn})](ClO_4)_2$ at 225 K along with the best fit to a single-exponential decay. Clearly, a single-exponential model is inadequate for describing the kinetics of this complex at 225 K. The data can be fit with a double exponential of the form

$$\Delta(OD) = A \exp\left(-\frac{t}{\tau_1}\right) + B \exp\left(-\frac{t}{\tau_2}\right) \qquad (2)$$

where τ_1 and τ_2 are the observed lifetimes of the two components of the biexponential decay. A fit of the data at 225 K to eq 2 with lifetimes of τ_1 = 124 ns and τ_2 = 776 ns is shown in Figure 6. The biphasic kinetics were found to be independent of both pump and probe wavelength across the entire $^1MLCT \leftarrow {}^1A_1$ absorption band. When we reexamined the data at 191 K using eq 2, a superior fit was obtained with τ_1 = 396 ns and τ_2 = 4880 ns; this value for τ_2 is not reliable since it implies we have fit on only ~20% of the half-life of the decay. The lack of clear, biphasic kinetics in our data at the lowest temperatures is strictly an artifact due to limitations of our equipment and does not reflect a characteristic of the chemical system.[21] The biphasic kinetics are in evidence on our apparatus at temperatures up to 260 K, whereupon it becomes apparent that a single exponential is once again adequate to describe the data.

Two points should be raised concerning the biexponential data discussed above. Fitting these data to a biexponential model was more difficult than fitting the single-exponential decays observed for the other systems.[11] The problems originate from the fact that we are instrumentally limited to time scales of ≤ 1 μs, implying that we will observe less than 1 half-life of any transient having $\tau > 1$ μs. In fitting data to eq 2, it is anticipated that the values for τ_1 and τ_2 will be correlated. The effect of this correlation would be to lower our confidence in the values obtained for τ_1 at temperatures where $\tau_2 > 1$ μs. However, truncation of the data set to include only those data for which τ_1, $\tau_2 \leq 1$ μs results in a change in the activation parameters of the τ_1 component of less than 5% (vide infra). Although we might have anticipated a larger effect, the sizable activation energy for the slow component means that τ_2 will be very long at low temperatures (e.g., ≈11 μs at 191 K). As a result, there will be little or no temporal evolution of τ_2 on the time scale of τ_1, so very little effect on the value of τ_1 is observed despite the fact that τ_2 is not well-determined. Second, as was mentioned above, we have not examined the temperature dependence of the magnetic susceptibility of $[Fe(t\text{-tpchxn})](ClO_4)_2$ in CH_3OH. We are therefore not in a position to calculate k_{-1} according to eq 3 for temperatures at which $K_{eq} \neq 0$. To circumvent this problem, we have chosen to analyze the data and obtain activation parameters from a truncated data set, including only those data for which $T \leq 250$ K. In this temperature regime, we are confident that setting K_{eq} = 0 in eq 3 is reasonable and will in any event introduce an error of only a few percent for the highest-temperature data points.

$$k_{-1} = \frac{k_{obs}}{K_{eq} + 1} \qquad (3)$$

(20) Purcell, K. F. *J. Am. Chem. Soc.* **1979**, *101*, 5147.

(21) Due to limitations with our equipment, we are only able to probe out to 1 μs, full scale. Given a longer pulse width flashlamp, the biphasic nature of the kinetics would be clearly evident at 190 K as well.

The *full* data set collected in the range 190–280 K is listed in Table III. A plot of $\ln(k)$ versus T^{-1} for both the τ_1 and τ_2 processes in the 190–250 K range is shown in Figure 7. The activation parameters for τ_1 are $E_a = 964 \pm 23$ cm^{-1} with a frequency factor of $(3.7 \pm 0.5) \times 10^9$ s^{-1}. For τ_2, we find $E_a = 2370 \pm 60$ cm^{-1} with a frequency factor of $(5 \pm 2) \times 10^{12}$ s^{-1}. Given the more than factor of 2 difference in the activation energies for the two processes, it follows that the two $\ln(k)$ versus T^{-1} curves will cross at some temperature. Setting the expressions from the $\ln(k)$ versus T^{-1} linear regressions to be equal, we calculate this crossing point to be $T \simeq 280$ K. This convergence of the two rates as predicted by the low-temperature data is nicely consistent with the experimentally observed collapse of the data to a single exponential in the temperature range 260–280 K. Although we are unable to collect data above 300 K, we would anticipate that the biexponential behavior would reemerge concurrent with the divergence of the kinetics of the two processes above 280 K with $\tau_2 < \tau_1$.

It was assumed in the above analysis that both of these kinetic processes are due to $^5T_2 \rightarrow {}^1A_1$ spin conversions. However, the uniqueness of the biphasic decay exhibited by [Fe(*t*-tpchxn)]-$(ClO_4)_2$ relative to the data obtained for all other Fe^{II} complexes requires that we consider other alternatives, as well. It seems clear on the basis of the observed bleaching of the $^1MLCT \leftarrow {}^1A_1$ absorption band and the *general* similarity of [Fe(*t*-tpchxn)]-$(ClO_4)_2$ to other complexes in the "tpen" series that at least one of the observed kinetic processes is associated with the $^5T_2 \rightarrow {}^1A_1$ relaxation. Given the fact that the activation energy for τ_1 is similar to those found[11] for [Fe(tpen)]$(ClO_4)_2$ and [Fe(tptn)]-$(ClO_4)_2$, it would be reasonable to ascribe τ_1 to the $^5T_2 \rightarrow {}^1A_1$ conversion. One possibility for τ_2 in terms of a parallel reaction pathway is ligand dissociation. This is a consideration, particularly in light of the positive value for $\Delta V^{\ddagger}$ observed by McGarvey et al.[12] for this system in DMF solution. McGarvey et al.[12] also considered ligand dissociation to explain their data but indicated that it was extremely unlikely given that these hexadentate ligands exhibit large formation constants ($K_f \approx 10^{14}$) and show strong resistance to dissociation under conditions of acid hydrolysis.[4a] We also think that it is unlikely that τ_2 corresponds to dissociation of part of the ligand framework. First, the resulting five-coordinate species (or solvent-ligated six-coordinate species) would be thermodynamically stable in the high-spin form. This type of complex would not show any propensity to relax to a low-spin isomer if thermalization is faster than τ_2^{-1}. In addition, we would expect that the species formed following dissociation of one of the pyridylmethyl arms of *t*-tpchxn would exhibit absorption properties distinct from the intact six-coordinate molecule, yet the kinetics (in particular the ratio of preexponential terms for τ_1 and τ_2) was found to be independent of probe wavelength. A sequential reaction pathway with τ_2 corresponding to ligand dissociation is also unlikely, since dissociation would likely precede the spin change. This would result in there being a rise time in the τ_1 component if it were observed at all under conditions where τ_2 is the rate-limiting step. This is not observed experimentally.

Another possibility for there being biphasic kinetics from a single, stepwise reaction pathway assigns τ_1 as ligand dissociation and τ_2 as the $^5T_2 \rightarrow {}^1A_1$ spin-state conversion. Again we point out the comments by McGarvey et al.[12] indicating that ligand dissociation in these systems is very difficult to achieve even under acidic conditions. However, one could envision a process whereby formation of the $^5T_2$ state occurs via pyridylmethyl arm dissociation to form a five-coordinate or solvent-bound species. Ligand rebinding kinetics are then described by τ_1, and the subsequent spin change is given by τ_2. This process would also result in there being a rise time for τ_2, but when combined with the decay from τ_1, this rise time might be difficult to detect. Solely on the basis of the nanosecond data, we cannot unequivocally rule this possibility out except to raise the point concerning the probe-wavelength independence of the observed kinetics (vide supra). In separate work,[22] we have studied the sub-picosecond dynamics (~500-fs pulse) of this complex and have found that the $^5T_2$ state is formed in less than 700 fs and thermalized within 3 ps following $^1MLCT \leftarrow {}^1A_1$ excitation. It is unlikely that ligand dissociation and thermalization of either a five-coordinate or six-coordinate solvent-bound species occurs on such a short time scale. In addition, it is very unlikely that the five-coordinate intermediate can be formed *after* thermalization since the energy of the molecule in the $^5T_2$ state will be below the thermodynamic threshold for ligand dissociation. We therefore believe that ligand dissociation is *not* contributing to the biphasic kinetics observed in [Fe(*t*-tpchxn)]$(ClO_4)_2$ and that both τ_1 and τ_2 are due to $^5T_2 \rightarrow {}^1A_1$ conversion processes.

Molecular Mechanism of $^5T_2 \rightarrow {}^1A_1$ Relaxation Processes. The τ_1 and τ_2 relaxation processes are assigned each as a $^5T_2 \rightarrow {}^1A_1$ relaxation. However, our data appear to be in conflict with the results of McGarvey et al.,[12] who observed simple monophasic kinetics in the temperature range 240–300 K. It has already been pointed out that the $^5T_2 \rightarrow {}^1A_1$ relaxation observed by McGarvey et al.[12] is markedly different in DMF as compared to CH_3CN. If the activation enthalpies reported by them are compared to those we obtained, a rather curious trend is found. The value for $\Delta H^{\ddagger}$ of the τ_2 component, 2205 ± 61 cm^{-1}, is similar to that found in DMF by McGarvey et al. ($\Delta H^{\ddagger} = 2876 \pm 100$ cm^{-1}). The activation enthalpy for τ_1 is significantly larger than that observed by them for $[Fe(t\text{-tpchxn})]^{2+}$ in CH_3CN (812 ± 23 cm^{-1} vs 150 ± 33 cm^{-1}) but still reflects the large disparity that exists between the two kinetic components. As such, it is reasonable to suggest that the biphasic kinetics that we observe in CH_3OH is a *combination* of the relaxation kinetics observed by McGarvey et al. for the same complex in DMF and CH_3CN. In other words, we agree with McGarvey et al. that the solvent is having an effect on the $^5T_2 \rightarrow {}^1A_1$ relaxation kinetics. In DMF, the solvation energies are such that one extreme is observed, whereas, in CH_3CN, some other high-spin form is stabilized. We suggest that our data in CH_3OH result from solvation properties that are intermediate between those in DMF and CH_3CN. Two different high-spin forms (i.e., $^5T_2$ complexes) are present, and this leads to the observation of biphasic decay kinetics for the $^5T_2 \rightarrow {}^1A_1$ relaxation. The intermediate nature of the CH_3OH solution of [Fe(*t*-tpchxn)]$(ClO_4)_2$ is further supported by the values we obtained for the activation enthalpies. In the case of the "DMF form" of the complex, the CH_3OH solution gives a slightly smaller value, and the "CH_3CN form" gives a slightly larger value, yet the *sum* of $\Delta H^{\ddagger}$ for τ_1 and τ_2 is nearly identical to the sum of $\Delta H^{\ddagger}$ for the DMF and CH_3CN solvent media.

It seems clear there exist *two* high-spin forms of this complex. These different forms can be stabilized under different conditions of solvation and exhibit markedly different barriers to spin-state interconversion as measured in solution. The question now is, What is the nature of these two forms? It is reasonable to conclude that the distinction must somehow be linked to the cyclohexylene ring, since this is the only substantial difference that exists between [Fe(*t*-tpchxn)]$(ClO_4)_2$ and molecules such as [Fe(tpen)]$(ClO_4)_2$ and [Fe(tppn)]$(ClO_4)_2$ for which only monophasic kinetics have been observed.[11] It is suggested that the difference between the two high-spin forms of [Fe(*t*-tpchxn)]$(ClO_4)_2$ has to do with a conformational change in the cyclohexylene ring. For example, one possibility is a conversion between the chair form found in the X-ray structure and a twisted-boat form that can be stabilized under certain conditions. Molecular models suggest that this interconversion can be carried out *without* the need for ligand dissociation of any kind. Alternatively, there may be a second chair configuration that is formed upon relaxation in the high-spin state that is less stable than the ground-state configuration, but conversion back requires a twisted-boat intermediate. This would

(22) (a) McCusker, J. K.; Walda, K. N.; Dunn, R. C.; Simon, J. D.; Magde, D.; Hendrickson, D. N. *J. Am. Chem. Soc.* **1992**, *114*, 6919. (b) McCusker, J. K.; Walda, K. N.; Dunn, R. C.; Simon, J. D.; Magde, D.; Hendrickson, D. N. *J. Am. Chem. Soc.* **1993**, *115*, 298.

(23) (a) Weaver, M. J.; McManis, G. E., III *Acc. Chem. Res.* **1990**, *23*, 294. (b) Weaver, M. J. *Chem. Rev.* **1992**, *92*, 368.

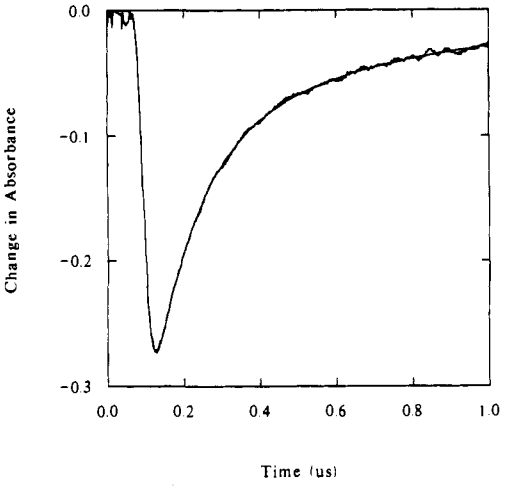

Figure 6. Transient decay profile of $[Fe(t\text{-tpchxn})](ClO_4)_2$ in CH_3OH (2.51×10^{-4} M) at 420 nm following excitation at 440 nm. Data were collected at 225 K. The smooth solid line represents a convolution of the instrument response function with a biexponential decay model. The two lifetimes are $\tau_1 = 124$ ns and $\tau_2 = 776$ ns.

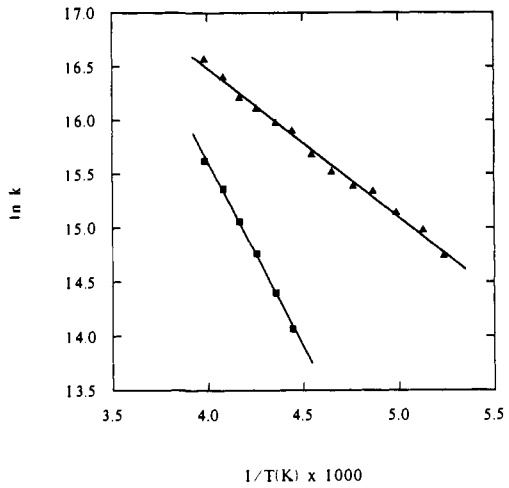

Figure 7. Arrhenius plot of relaxation data for $[Fe(t\text{-tpchxn})](ClO_4)_2$ collected in CH_3OH at a concentration of 2.51×10^{-4} M. The two data sets are for τ_1 (▲) and τ_2 (■). The solid line represents a best-fit linear least-squares regression of the data; see Table III for details.

be consistent with the positive value for $\Delta V^{\ddagger}$ observed by McGarvey et al.,[12] since activation from a chair to a twisted boat will involve a small increase in molecular volume.

The overall process is envisioned to occur in the following way. The $[Fe(t\text{-tpchxn})]^{2+}$ complex in a CH_3OH medium is first excited to the ^{1}MLCT excited state. From our previous studies,[22] it is known that this complex, and for that matter all low-spin Fe^{II} complexes studied, intersystem-crosses to the $^5T_2$ state in less than ~700 fs. It is also believed[22] that it takes only 2–3 ps to vibrationally cool in the $^5T_2$ state. Thus, in the short time (~700 fs) that it takes for the complex to make the ^{1}MLCT $\rightarrow$ $^5T_2$ intersystem crossing, the CH_3OH solvent structure influences the conformation of the $[Fe(t\text{-tpchxn})]^{2+}$ complex. One form of the complex develops in less than ~700 fs which has the cyclohexylene ring in a chair conformation. The other form of the complex also develops in less than ~700 fs and probably has the cyclohexylene ring in another conformation. The two different forms of the complex then thermalize and undergo the $^5T_2 \rightarrow {}^1A_1$ relaxation at different rates.

If molecular motion accompanying the spin change were to proceed along a predominantly torsional coordinate, then it would be anticipated that a conformational change in the cyclohexylene ring structure in $[Fe(t\text{-tpchxn})]^{2+}$ accompanies the $^5T_2 \rightarrow {}^1A_1$ intersystem crossing. It is difficult to predict which form of the molecule would produce a greater barrier to spin-state relaxation,

Table III

Relaxation Data for $[Fe(t\text{-tpchxn})](ClO_4)_2$ in CH_3OH at 2.51×10^{-4} M (3.18×10^{-4} *m*)

temp (K)[a]	τ_{obs}(ns)[b]	$k_{-1}(s^{-1})$[c]	temp (K)[a]	τ_{obs}(ns)[b]	$k_{-1}(s^{-1})$[c]
191	396	2.53×10^6	235	101	9.90×10^6
	4880[d]			388	2.58×10^6
195	313	3.19×10^6	240	91.4	1.09×10^7
	1440[d]			288	3.47×10^6
200	266	3.76×10^6	245	75.5	1.32×10^7
	2650[d]			212	4.72×10^6
205	218	4.59×10^6	251	63.7	1.57×10^7
	1560[d]			164	6.10×10^6
210	208	4.81×10^6	255	53.1	1.88×10^7
	3610[d]			153	6.54×10^6
215	182	5.49×10^6	260[e]	96.6	1.04×10^7
	1890[d]		265	85.6	1.17×10^7
220	155	6.45×10^6	271	68.2	1.47×10^7
	1490[d]		275	64.1	1.56×10^7
225	124	8.06×10^6	280	61.8	1.62×10^7
	776	1.29×10^6			
230	115	8.70×10^6			
	558	1.79×10^6			

Linear Regression Analyses[f]

model	slope	intercept	correlation
Arrhenius (ln(k))	−1386 ± 34	22.0 ± 0.15	0.994
	−3410 ± 86	29.3 ± 0.4	0.997
Eyring (ln(k/T))	−1169 ± 33	15.6 ± 0.15	0.992
	−3172 ± 88	22.8 ± 0.4	0.997

Activation Parameters

Arrhenius	$E_a = 96.4 \pm 23$ cm^{-1}	$A = 3.7 \pm 0.5 \times 10^9$ s^{-1}
	$E_a = 2370 \pm 60$ cm^{-1}	$A = 5 \pm 2 \times 10^{12}$ s^{-1}
Eyring	$\Delta H^{\ddagger} = 812 \pm 23$ cm^{-1}	$\ln(\kappa) + \Delta S^{\ddagger}/R = -8.2 \pm 0.1$
	$\Delta H^{\ddagger} = 2205 \pm 61$ cm^{-1}	$\ln(\kappa) + \Delta S^{\ddagger}/R = -1.0 \pm 0.1$

[a] Relative error bars for the temperature are estimated to be ±1 K; the absolute error is ±2 K. [b] Lifetimes are accurate to ca. 5–7%. [c] Calculated assuming $K_{eq} = 0$. [d] Values for $\tau_{obs} > 1$ μs are not reliable; see text for further details. [e] For $T \geq 260$ K, a single exponential was sufficient to model the observed decay. [f] Based on data from biexponential fits for $T \leq 250$ K.

i.e., which of τ_1 and τ_2 is due to a given conformation. Since the X-ray structure indicates a chair configuration, a change to a twisted-boat form would introduce an additional barrier to ground-state recovery that would increase the observed activation energy for the $^5T_2 \rightarrow {}^1A_1$ process; this could be assigned as τ_1. In the case of τ_2, a chair form that is somehow distinct from the ground-state structure would require the formation of a twisted-boat intermediate and would likely cause a substantial increase in the activation energy for the $^5T_2 \rightarrow {}^1A_1$ relaxation. Regardless of these details, we wish to point out that *any* kind of a distinct conformational change along a torsional coordinate would fit well with the model developed in our previous study[11] whereby geometric preferences of the ligand can *induce* the system to proceed further along the reaction coordinate than is minimally necessary to achieve a spin change. This gives rise to more dynamical mixing of the $S = 0$ and $S = 2$ spin manifolds and a larger intrinsic rate for spin-state interconversion. In this context, the frequency factor of $(5 \pm 2) \times 10^{12}$ s^{-1} for $[Fe(t\text{-tpchxn})](ClO_4)_2$ is of interest, since it is a full 2 orders of magnitude larger than that found for $[Fe(tptn)](ClO_4)_2$ despite the lower energy of the $^5T_2$ state in $[Fe(t\text{-tpchxn})](ClO_4)_2$.

Both of these scenarios place the role of the solvent in the forefront since they require stabilization of a particular conformation of the molecule as the system relaxes in the high-spin state. Although this is certainly consistent with the available data, we have very little information on the nature of solvation and solvent dynamics in these types of systems. As a result, it is difficult to comment on whether or not solvent-induced conformational changes of the type we are suggesting are at all reasonable. It is curious to note, however, that the frequency factor for the high-energy process in $[Fe(t\text{-tpchxn})](ClO_4)_2$ is approaching a value where solvent dynamics may play a critical role.[23]

Acknowledgment. We are grateful for funding from NSF Grant CHE-9115286 and NIH Grant HL-13652.

Supplementary Material Available: Tables of crystallographic data, bond distances and angles, anisotropic displacement coefficients, calculated hydrogen atom coordinates, magnetic susceptibility data, and positional parameters for $[Fe(t\text{-tpchxn})](ClO_4)_2 \cdot H_2O \cdot CH_3OH$ (10 pages); a listing of observed and calculated structure factors (9 pages). Ordering information is given on any current masthead page.

High-Spin Molecules: $[Mn_{12}O_{12}(O_2CR)_{16}(H_2O)_4]$

Roberta Sessoli,[1] Hui-Lien Tsai,[2] Ann R. Schake,[3a] Sheyi Wang,[3a] John B. Vincent,[3a] Kirsten Folting,[3b] Dante Gatteschi,*[,1] George Christou,*[,3a] and David N. Hendrickson*[,2]

Contribution from the Department of Chemistry-0506, University of California at San Diego, La Jolla, California 92093-0506, Dipartimento di Chimica, Università di Firenze, 50144 Firenze, Italy, and Department of Chemistry and Molecular Structure Center, Indiana University, Bloomington, Indiana 47405. *Received September 18, 1992*

Abstract: The syntheses and electrochemical and magnetochemical properties of $[Mn_{12}O_{12}(O_2CPh)_{16}(H_2O)_4]$ (**3**), its solvate **3**·$PhCOOH \cdot CH_2Cl_2$, and $[Mn_{12}O_{12}(O_2CMe)_{16}(H_2O)_4] \cdot MeCOOH \cdot 3H_2O$ (**4**) are reported. Complex **3** can be prepared either by reaction of $Mn(OAc)_2 \cdot 4H_2O$, benzoic acid, and $NBu^n_4MnO_4$ in pyridine or by reaction of PhCOOH with complex **4** slurried in CH_2Cl_2. Complex **3** crystallizes in the triclinic space group $P\bar{1}$, which at −146 °C has a = 27.072(19) Å, b = 17.046(11) Å, c = 14.254(8) Å, α = 98.39(3)°, β = 98.44(4)°, γ = 89.27(4) Å, and Z = 2. The structure was refined with 4814 observed $[F > 3.0\sigma(F)]$ reflections to give R = 9.54 and R_w = 10.07. $[Mn_{12}O_{12}(O_2CPh)_{16}(H_2O)_4]$ (**3**) consists of a central $[Mn^{IV}_4O_4]^{8+}$ cubane held within a nonplanar ring of eight Mn^{III} atoms by eight μ_3-O^{2-} ions. Peripheral ligation is provided by 16 μ_2-O_2CPh^- and four terminal H_2O groups, where the four H_2O ligands are located on two Mn atoms. Four redox waves are seen in the cyclic voltammogram of complex **3** in CH_2Cl_2: two reversible waves [an oxidation wave at 0.79 V (vs ferrocene/ferrocenium) and a reduction wave at 0.11 V] and two irreversible waves at −0.23 and −0.77 V. Complex **4** exhibits the same four redox couples in MeCN. Variable-temperature DC magnetic susceptibility data measured at 10.0 kG are presented for polycrystalline samples of complex **3** and the solvate **3**·$PhCOOH \cdot CH_2Cl_2$. At 320 K, μ_{eff}/molecule is ~12 μ_B and increases to a maximum of ~20–21 μ_B at ~10 K, whereupon μ_{eff}/molecule decreases rapidly at low temperatures. It is concluded that these complexes exhibit appreciable magnetic anisotropy. Even at fields as low as 1 kG the polycrystallites have to be restrained from torquing by embedding the polycrystalline sample in parafilm. Complexes **3** and **3**·$PhCOOH \cdot CH_2Cl_2$ exhibit somewhat different μ_{eff}/molecule versus temperature curves. Magnetization measurements at 20.0, 30.0, 40.0, and 50.0 kG in the 2–4 K range are used to determine that in these fields complexes **3** and **3**·$PhCOOH \cdot CH_2Cl_2$ have S = 10 and S = 9 ground states, respectively. A relatively large zero-field splitting is in evidence, and this was confirmed by high-field EPR experiments with a CO_2 far-infrared laser. AC susceptibility data in zero applied field are given for complexes **3** and **4** in the 4–25 K range. It is concluded that complex **3** has a S = 9 ground state at zero field, whereas complex **4** has a S = 10 ground state at zero field. The most interesting observation for complexes **3** and **4** derives from the out-of-phase (imaginary) component of the AC susceptibility, χ_M''. Both of these complexes exhibit a nonzero χ_M'', which when measured at various frequencies shows a maximum at different temperatures. These two complexes are the only molecular solids known to exhibit a nonzero χ_M'' in the paramagnetic phase. The results of theoretical calculations of the ordering of spin states in a $Mn_4^{IV}Mn_8^{III}$ complex, assuming reasonable values for the exchange parameters characterizing the different pairwise interactions, are presented to rationalize the S = 8–10 ground states.

Introduction

Considerable effort has been directed at understanding magnetic exchange interactions occurring in polynuclear transition-metal complexes.[4] The nature (antiferromagnetic or ferromagnetic) and magnitude of a magnetic exchange interaction between two metal ions are reasonably well understood in terms of the energetics and overlap of "magnetic orbitals".[4a] The success in understanding magnetic exchange interactions in polynuclear complexes has prompted efforts in the last few years to see if these complexes can be used as molecular building blocks for materials exhibiting interesting properties. In general, the concept of molecular-based materials is being pursued in many directions. Instead of using solids consisting of extended lattices such as in oxides, the goal is to make up a solid lattice of molecular building blocks. With certain building blocks arranged properly in a solid lattice, it may be possible to prepare a material that exhibits interesting properties. Examples of this molecular-based materials approach can be found in the active research on organic materials with nonlinear optical properties[5] and the studies on organic conductors and superconductors.[6]

Miller, Epstein, and co-workers[7] have prepared organometallic ferromagnets where metallocene cations (D^+) and organic anions (A^-), each with a single unpaired electron ($S = {}^1/_2$), are assembled in alternating stacks. The pairwise ($D^+ \cdots A^-$) magnetic exchange interactions in each stack are important, but it is the exchange

(1) Università di Firenze.
(2) University of California at San Diego.
(3) (a) Department of Chemistry, Indiana University. (b) Molecular Structure Center, Indiana University.
(4) (a) *Magneto-Structural Correlation in Exchange-Coupled Systems*; Willett, R. D., Gatteschi, D., Kahn, O., Eds.; NATO ASI Series C, 140; D. Reidel Publishing Co.: Dordrecht, The Netherlands, 1985. (b) *Magnetic Molecular Materials*; Gatteschi, D., Kahn, O., Miller, J. S., Palacio, F., Eds.; NATO ASI Series E, 198; Kluwer Academic Publishers: Dordrecht, The Netherlands, 1991.
(5) (a) *Nonlinear Optical Properties of Organic Molecules and Crystals*; Chemla, D. S., Zyss, J., Eds.; Academic Press: Orlando, 1987; Vols. 1 and 2. (b) Williams, J. M. *Angew. Chem., Int. Ed. Engl.* **1984**, *23*, 690. (c) *Materials for Nonlinear Optics, Chemical Perspectives*; Marder, S. R., Sohn, J. E., Stucky, G. D., Eds.; ACS Symposium Series 455; American Chemical Society: Washington, DC, 1991.
(6) (a) Bredas, J. L.; Street, G. B. *Acc. Chem. Res.* **1985**, *18*, 309. (b) Wudl, F. *Acc. Chem. Res.* **1984**, *17*, 227. (c) Torrance, J. B. *Acc. Chem. Res.* **1979**, *12*, 79. (d) Williams, J. M. *Prog. Inorg. Chem.* **1985**, *33*, 183.
(7) (a) Miller, J. S.; Epstein, A. J.; Reiff, W. M. *Chem. Rev.* **1988**, *88*, 201 and references therein. (b) Miller, J. S.; Epstein, A. J.; Reiff, W. M. *Acc. Chem. Res.* **1988**, *21*, 114 and references therein.

0002-7863/93/1515-1804$04.00/0